Title
Broad-specificity GH131 β-glucanases are a hallmark of fungi and oomycetes that colonize plants

Journal
Environmental Microbiology, 21(8)

ISSN
1462-2912

Authors
Anasontzis, George E
Lebrun, Marc-Henri
Haon, Mireille
et al.

Publication Date
2019-08-01

DOI
10.1111/1462-2920.14596

Peer reviewed

Broad-specificity GH131 β-glucanases are a hallmark of Fungi and Oomycetes that colonise plants

Running title: Fungal GH131s, key enzymes in plant-cell-wall remodelling

George E. Anasontzis[1,2,§], Marc-Henri Lebrun[3], Mireille Haon[1], Charlotte Champion[1], Annegret Kohler[4], Nicolas Lenfant[2], Francis Martin[4], Richard J. O'Connell[3], Robert Riley[5], Igor V. Grigoriev[5,6], Bernard Henrissat[2,7], Jean-Guy Berrin[1], Marie-Noëlle Rosso[1,*]

[1]INRA, Aix-Marseille Univ, UMR1163, Biodiversité et Biotechnologie Fongiques, BBF, Marseille, France ;

[2]CNRS, Aix-Marseille Univ, UMR7257, Architecture et Fonction des Macromolecules Biologiques, Marseille, France ;

[3]INRA, AgroParisTech, Université Paris-Saclay, BIOGER, Thiverval-Grignon, France;

[4]INRA, University of Lorraine, Laboratory of Excellence Advanced Research on the Biology of Tree and Forest Ecosystems (ARBRE), UMR 1136, Champenoux, France;

[5]US Department of Energy Joint Genome Institute (JGI), Walnut Creek, California, USA;

[6]Department of Plant and Microbial Biology, University of California Berkeley, Berkeley, CA 94598, USA;

[7]INRA, USC 1408, AFMB, Marseille, France;

*Corresponding author: Dr. Marie-Noëlle Rosso, marie-noelle.rosso@inra.fr

§ Current address: George E. Anasontzis, DTU Bioengineering, Technical University of Denmark, Kongens Lyngby, Denmark

Originality-Significance Statement

GH131 is a recently discovered fungal family of Glycoside Hydrolases, which we also identified in Oomycetes, but not in other eukaryotes. Our evolutionary analyses and functional characterisation pointed out a correlation between the presence of GH131 fungal enzymes in the genome of a microbe and its (plant-associated) lifestyle. This correlation across Dikarya suggests a significant role of GH131 in the adaptation of fungi to land plants.

Our results suggest that GH131s contribute to plant tissue colonisation by fungi, whatever the degree of plant-cell-wall deconstruction required for establishment of the plant-fungus interaction. We propose that GH131s are secreted by these fungi to unlock the plant cell wall structure and allow plant-cell-wall remodelling or disruption during plant-tissue colonisation by fungal hyphae.

Summary

Plant-tissue-colonising fungi fine-tune the deconstruction of plant-cell walls (PCW) using different sets of enzymes according to their lifestyle. However, some of these enzymes are conserved among fungi with dissimilar lifestyles. We identified genes from Glycoside Hydrolase family GH131 as commonly expressed during plant-tissue colonisation by saprobic, pathogenic, and symbiotic fungi. By searching all the publicly available genomes, we found that GH131-coding genes were widely distributed in the Dikarya subkingdom, except in Taphrinomycotina and Saccharomycotina, and in phytopathogenic Oomycetes, but no other eukaryotes nor prokaryotes. The presence of GH131 in a species was correlated with its association with plants as symbiont, pathogen, or saprobe. We propose that GH131-family expansions and horizontal-gene transfers contributed to this adaptation. We analysed the biochemical activities of GH131 enzymes whose genes were up-regulated during plant-tissue colonisation in a saprobe (*Pycnoporus sanguineus*), a plant symbiont (*Laccaria bicolor*), and three hemibiotrophic-plant pathogens (*Colletotrichum higginsianum*, *C. graminicola*, *Zymoseptoria tritici*). These enzymes were all active on substrates with β-1,4, β-1,3, and mixed β-1,4/1,3 glucosidic linkages. Combined with a cellobiohydrolase, GH131 enzymes enhanced cellulose degradation. We propose that secreted GH131 enzymes unlock the PCW barrier and allow further deconstruction by other enzymes during plant tissue colonisation by symbionts, pathogens and saprobes.

Keywords: cellulase, ectomycorrhizal fungi, saprotrophic fungi, phytopathogenic fungi, symbiotic fungi, plant cell wall degradation.

Introduction

The emergence of land plants between 500 and 700 million years ago (Heckman et al. 2001) involved modifications of their cell wall (PCW) which occurred simultaneously with the occurrence of novel biotic interactions with terrestrial fungi (de Vries et al., 2018; Lutzoni et al., 2018). During this plant - fungal co-evolution, early terrestrial fungal lineages have likely acquired the ability to use plant tissues as nutrient source either as saprobes, symbionts/mutualists, or pathogens (Chang et al. 2015; Berbee et al. 2017). All these fungal lifestyles require modifications of PCWs, the natural barrier that protects plant cells from external threats. The extent of PCW modification or disruption is the direct result of the fine-tuned secretion of specialised sets of enzymes active on these polymers (Gan et al. 2013). Saprotrophic fungi fully decompose PCW as they progress into dead plant tissues, while symbiotic fungi only partially modify PCW to facilitate nutrient exchanges with living plant cells (Balestrini and Bonfante, 2014). In particular, ectomycorrhizal symbiotic fungi have lost most of the genes encoding PCW-degrading enzymes found in related saprotrophic fungi (Veneault-Fourrey and Martin 2011; Zhao et al. 2013; Kohler et al. 2015). Hemi-biotrophic pathogenic fungi first colonise plant tissues with moderate or highly localized host-PCW modifications, before switching to a necrotrophic phase that causes extensive PCW degradation.

PCW is a matrix of cross-linked cellulose, hemicellulose, and pectin networks, glycosylated proteins, and lignin (Cosgrove 2005). Although there are significant differences in PCW composition between gymnosperms and angiosperms, between dicotyledons and monocotyledons and between different tissues of a same plant (Leroux et al. 2015), cellulose is invariably a crucial component of PCW. It consists of linear chains of several hundred to over ten thousand β-1,4-linked D-glucose units. In PCWs, cellulose microfibrils occur as insoluble cable-like structures that are typically composed of about 36 hydrogen-bonded glucan chains. The crystalline cellulose core of micro-fibrils is strengthened by strong interchain hydrogen bonds and by a protective layer of hemicellulose that make crystalline cellulose resistant to enzymatic hydrolysis (Beckham et al., 2011; Ritter 2008; Couturier et al., 2018). Cellulose degradation by fungi involves combinations of enzymes such as Glycoside Hydrolase (GH) family 5 (GH5), GH6, GH7, GH12, and GH45, which display either endo-β-1,4-glucanase or cellobiohydrolase

(CBH) activities, as well as GH1 and GH3 β-glucosidases. Cellulose is also degraded by oxidative cleavage by enzymes of family AA9 (Lytic Polysaccharide Monooxygenases, LPMOs, Gupta et al. 2016; Berrin et al. 2017). Additional enzymes are also likely to be involved in cellulose degradation. The less-studied GH131 family (Lafond et al. 2012) is a good candidate for being a component of the cellulose degrading enzymatic complex. Indeed, the GH131 from the coprophilic fungus *Podospora anserina* (*Pa*Gluc131A) displayed an endo-activity on β-(1,4)-glucan oligomers and mixed β-(1,3;1,4)-oligosaccharides, although with a low specific activity on the latter substrates. However, no other member of the GH131 family has been characterized to date and no data is available on the occurrence of these enzymes in the Tree of Life. To decipher the role of GH131 enzymes in PCW modification, we used a combination of phylogenetic analyses, comparative analysis of available transcriptome data, and biochemical characterisation of different recombinant GH131 enzymes. We searched for the presence of GH131-coding genes in all available fungal genomes and beyond, in the genomes from other microorganisms. The widespread occurrence of GH131 in Dikarya and Oomycetes feeding on plants suggested their importance in PCW modification. Comparative transcriptomics, using data from model fungi with different lifestyles (plant saprobes, pathogens, and symbionts), highlighted in each fungal species at least one GH131-coding gene up-regulated during plant colonisation. We expressed these *in planta* up-regulated genes in *Pichia pastoris*, and showed a broad range specificity of the respective recombinant enzymes towards β-1,3 and β-1,4 glucosidic bonds. Taken together, our results suggest that GH131 enzymes have contributed to the adaptation of fungal and oomycete species to a lifestyle associated with plant tissue colonisation and PCW modifications.

Results

GH131-coding genes are widespread among fungi and oomycetes living on plant tissues

To acquire an overall vision on the distribution of GH131 genes in living organisms, we browsed all finished genomes available on Genbank (last accessed on July 02, 2017). These included seven protists, two Amoebozoa, 42 SAR (Stramenopile, Alveolata, Rhizaria), 10 Excavata, 17 Viridiplantae, 56 Animalia), about 10,000 Bacteria and 300 Archaea. For Fungi, we also analysed the genomes publicly available on the JGI Mycocosm portal (https://genome.jgi.doe.gov/programs/fungi/index.jsf, last accessed on July 02, 2017). GH131-coding genes were absent from all taxa except Fungi and Oomycota. GH131-coding genes were identified in 56% of the 801 analysed fungal genomes, and in seven plant-associated oomycetes (Table S1 in supplementary material). GH131-coding genes were absent from genomes of all Early Diverging Fungi (e.g. Zoopagomycota, Blastocladiomycota, Microsporidia), except *Gonapodya prolifera* (Chytridiomycota). On the contrary, GH131-coding genes were present in 60% of the Dikarya (Basidiomycota and Ascomycota) genomes. In Basidiomycota, GH131-coding genes were found in Agaricomycotina and in Pucciniales, but not in Ustilagomycotina. Among Ascomycota, GH131 genes were detected in species from Pezizomycotina and were absent from all species from the basal sub-phyla Taphrinomycotina and Saccharomycotina (Fig. 1; Table S1).

GH131 gene copy numbers were highly variable across Fungi. For example, within Ascomycetes, GH131 gene copy numbers were higher in Magnaporthales (6 gene copies in each *Magnaporthe oryzae* and *M. poae* genomes) than in Hypocreales (1 single gene copy in *Fusarium* genomes analysed). GH131 gene copy numbers within taxonomic orders were generally homogeneous, except in a few cases such as Glomerellales in which it varied from 8 in the genus *Colletotrichum*, to 2 in *Verticillium* (Fig. 1; Table S1). Gene tree-species tree reconciliation suggested that GH131 gene family expansions occurred independently in Ascomycetes and Basidiomycetes (Fig. 1). In Ascomycetes, gene family expansions possibly occurred in a common ancestor of Pezizomycotina and were particularly abundant in the ancestor lineage of Sordariomycetes. In Basidiomycetes, the largest GH131 gene families were found

in Pucciniomycetes (9 gene copies in *Melampsora larici-populina*, 7 gene copies in *Puccinia striiformis*) and gene family expansions supposedly occurred within Agaricomycetes lineages.

The absence of GH131-coding genes in the genomes of Early Diverging Fungi suggested that GH131 first occurred in a common ancestor of Dikarya. One single exception was the presence of a GH131 gene in the chytridiomycete *Gonapodya prolifera.*. Outside the fungal kingdom, GH131-coding genes were only observed in Oomycota from genera *Pythium* and *Phytophthora*. Oomycetes are Stramenopiles microorganisms within Stramenopiles-Alveolata-Rhizaria (SAR) eukaryotic supergroup. No GH131-coding genes were found among all other Stramenopiles surveyed; *Schizochytrium aggregatum*, *Aplanochytrium kerguelense*, *Aurantiochytrium limacinum*, Ochromonadaceae sp., *Blastocystis* sp., *Ectocarpus siliculosus*, *Paraphysomonas imperforata*, *Achlya hypogyna*, *Thraustotheca clavata*, *Albugo laibachii*, *and four diatoms* (*Fragilariopsis cylindrus*, *Phaeodactylum tricornutum*, *Thalassiosira pseudonana*, *Minidiscus trioculatus*). Oomycetes are closely related to brown algae and therefore are phylogenetically distant from Fungi, despite sharing filamentous growth and osmotrophic (heterotrophic, absorptive) nutrition, likely independently acquired through convergent evolution (Baldauf et al., 2000, Cavalier-Smith and Chao, 2006). Setting the number of HGT allowed to 3 in the gene tree-species tree reconciliation study unveiled a potential HGT between a common ancestor of the Dikarya and a common ancestor of Pythiales and Peronosporales (Fig. 1).

For a phylogenetic analysis, we selected 197 sequences originating from 75 fungal and oomycetes species (Fig. 2). The phylogenetic analysis was performed using only the protein sequences corresponding to the GH131 catalytic module (Sup. Material). All GH131 sequences from oomycetes clearly grouped into a separate clade (Clade A, Fig. 2) suggesting an early divergence between fungal and oomycete GH131 genes from a common eukaryotic progenitor gene or an event of HGT between these taxa as suggested by the gene tree-species tree reconciliation (Fig. 1). Clades B and C contained GH131 sequences from both Basidiomycota and Ascomycota while Clade D contained only GH131 sequences from Basidiomycota with Pucciniomycetes and Agaricomycotina sequences forming two

distinct clades, as expected from independent evolution of common ancestor genes. Clade C also included the only GH131 sequence from an early diverging fungus (*G. prolifera*, Chytridiomycota) that clustered with sequences of the ascomycetes *Magnaporthiopsis poae* (#4609, with sequence similarity 52%) and *Magnaporthe oryzae* (#MGG_13993T0, with sequence similarity 50%). The clustering of these three GH131 sequences was further supported by additional phylogenetic analyses using Neighbour Joining and Maximum Parsimony (data not shown) which reinforced the hypothesis of an HGT from a Magnaporthales ancestor towards the *Gonapodya* lineage suggested by gene tree-species tree reconciliation analysis (Fig. 1). Recent GH131 gene family expansions were detected in Pucciniales (e.g. *Puccinia graminis*), in Agaricomycetes (e.g. *Tulasnella calospora*) and in Oomycetes (e.g. *Phytophthora infestans*) (Fig. 2).

Only Clade B included GH131 proteins with both a catalytic domain and an additional Carbohydrate Binding Module (CBM1). These GH131-CBM1 proteins were found in a wide range of species from both Basidiomycota and Ascomycota, with a discontinuous taxonomic distribution. Although these CBM1 protein sequences were related (same CBM1 Orthofinder family; data not shown), the resolution of their phylogenetic tree was poor, likely due to their small size (27-38 amino acids; Fig. S1 and Fig. S2 in supplemental material) and could not be used for inferring their evolution.

Distribution of GH131-coding genes across fungi with different lifestyles

Since the highest numbers of GH131 gene copies were observed in plant pathogens and plant endophytes, we searched for relationships between lifestyle and GH131 gene copy numbers per genome among 82 Dikarya fungal species with a defined lifestyle, excluding species from Saccharomycotina and Taphrinomycotina, which did not have GH131 genes (Table S1). GH131-coding genes were almost absent from insect- and mammal-associated species (AA for animal-associated fungi in Fig. 3). Exceptions in AA fungi come from two nematode pathogens (*Arthrobotrys oligospora* and *Dactylellina haptotyla*) and the opportunist human pathogen *Aspergillus fumigatus* that do carry two GH131-coding genes each (Fig. 3, Table S1). *A. oligospora* and *D. haptotyla* capture plant parasitic nematodes in the

rhizosphere and *A. fumigatus* is a saprobe on decaying plant tissues with the ability to switch to a human-pathogen lifestyle. As a common trait, these three species are soil dwelling fungi that can switch to saprophytic behavior (Latgé JP, 1999; Soares et al., 2018). Strikingly, 27 out of 29 plant-pathogenic Dikarya had at least one GH131. In addition, these species had the highest number of GH131-coding genes, with 8 GH131 genes in *Colletotrichum higginsianum* (Pezizomycotina, Ascomycota), 6 in *Rhizoctonia solani* (Agaricomycotina, Basidiomycota), and 9 in *Melampsora larici-populina* (Pucciniomycotina, Basidiomycota). The only plant pathogenic species that had no GH131 were two Ustilaginales species, which could be related to the absence of GH131 genes in the lineage Ustilagomycotina. Ten out of 12 genomes from plant symbiotic Dikarya carried at least one GH131, the maximum being observed in the endophyte *Phialocephala scopiformis* (Pezizomycotina, Ascomycota) with 6 GH131 genes. Finally, 30 out of 32 genomes from saprobic Dikarya carried at least one GH131, the maximum number of gene copies being observed in *Pseudomassariella vexata* (Xylariales, Ascomycota), with 5 GH131 genes. Overall, the presence of GH131 in the genome of a Dikarya species was strongly correlated with a plant-colonising lifestyle (saprobes, pathogens, and symbionts), with some exceptions (10% of these species had no GH131), while most (73%) of the animal-associated fungal species we analysed did not have any GH131. To further test the hypothesis that the GH131 gene copy number was correlated with plant-associated lifestyles, we merged all Dikarya species in four lifestyles, non-plant-associated (NR), symbiotic (SYM; including all mycorrhizal species and endophytes), plant pathogens (PP), and saprotrophs (S), and performed a phylogenetic generalised least squares analysis. Plant-associated lifestyles and GH131 gene copy numbers were fitted using the Ornstein-Uhlenbeck model under Martins correlation, with an alpha factor 3.17 and a p-value of 0.0021 for the plant-pathogenic lifestyle, 0.089 for the saprotrophs, and 0.07 for the symbionts (Table S2). This suggested that the co-occurrence of GH131 in recently diverged species, such as *A. brasiliensis* and *A. niger* (Fig. 1), was a result of their phylogenetic relationship, while among species with longer divergence time, the presence of GH131 was related with the plant-associated lifestyle.

203 **GH131-coding genes are up-regulated when fungi colonise plant tissues**

204 To investigate the biological role of GH131 enzymes in plant-colonising fungal lifestyles, we focused
205 on exemplar fungal species with three different lifestyles: three plant pathogens, *Colletotrichum*
206 *higginsianum*, *C. graminicola*, and *Zymoseptoria tritici*; three white-rot saprotrophic fungi, *Pycnoporus*
207 *sanguineus*, *P. coccineus*, and *P. cinnabarinus*; and one ectomycorrhizal symbiotic fungus, *Laccaria*
208 *bicolor*, taking advantage of available genomic and transcriptomic data from different infection stages
209 and/or substrates (Martin et al. 2008; Goodwin et al. 2011; O'Connell et al. 2012; Gan et al. 2013;
210 Levasseur et al. 2014; Veneault-Fourrey et al. 2014; Rudd et al. 2015; Miyauchi et al. 2016; Palma-
211 Guerrero et al. 2016) and, in the case of the plant pathogenic ones, their well-defined infection stages
212 (Perfect et al. 1999; Duncan and Howard 2000; O'Connell et al. 2004; Munch et al. 2008). The number
213 of genes coding for GH131 varied among the different species, from one in *L. bicolor* and *Z. tritici* to
214 more than seven in *Colletotrichum* species (Table 1). In each of the selected species, at least one GH131
215 gene copy was transcriptionally up-regulated during interaction with the host plant or during growth on
216 a plant substrate (Table 2). *L. bicolor* GH131-coding gene (Clade D, Fig. 2) was up-regulated more than
217 100-fold during ectomycorrhizal formation with poplar roots, compared to free-living mycelium. In *C.*
218 *higginsianum,* CH063_00647 (Clade C) was the most strongly up-regulated gene during both biotrophic
219 (100-fold) and necrotrophic phases (271-fold) compared to *in vitro* appressoria, whereas CH063_03177
220 (Clade C) was up-regulated earlier during appressorial penetration and the biotrophic phase (38-fold).
221 In *C. graminicola,* GLRG_10695 (Clade B), orthologous to *C. higginsianum* CH063_06244, was up-
222 regulated 6- and 7-fold during the biotrophic and necrotrophic phases respectively. The only *Z. tritici*
223 GH131-coding gene (Clade C) was up-regulated 56-fold during the asymptomatic phase and 27-fold
224 during the necrotrophic phase, compared to *in vitro* growth. When grown on aspen, the most highly
225 induced GH131-coding genes in *P. sanguineus* were #571793 (Clade B) and #1756265 (Clade D; 9.6-
226 fold and 11-fold respectively) and their orthologs in *P. coccineus*, #1467772 and #1376091 (Table S3).
227 In conclusion, at least one GH131-coding gene was up-regulated when each of these fungi colonise
228 plant tissues, regardless of their lifestyle.

229

GH131s from different fungal species and clades share similar substrate specificities

To compare substrate specificities across fungal GH131 proteins, we selected seven enzymes (*L. bicolor* *Lb*Gluc131A, *C. higginsianum* *Ch*Gluc131A and *Ch*Gluc131B, *C. graminicola* *Cg*Gluc131A, *P. sanguineus* *Ps*Gluc131A and *Ps*Gluc131B, *Z. tritici* *Zt*Gluc131A) based on (i) their gene expression patterns during plant colonisation (Table 2), (ii) the lifestyle of their carrying species (Table S1), and (iii) their phylogenetic relationships (Fig. 2). These genes were distributed among most Dikarya clades in the phylogram shown in Fig. 2. Apart from the *Ps*Gluc131A (#571793), which harbours a CBM1 in its native form, all the GH131 selected had no appended CBM1 module. The seven selected GH131-coding genes were expressed in *P. pastoris* and activities of the purified recombinant enzymes were assayed against a range of β-1,4, β-1,3, β-1,3/1,4, and β-1,6 glucan substrates *in vitro* (Table 3). *L. bicolor* *Lb*Gluc131A showed very low activity on phosphoric acid swollen cellulose (PASC) and long cello-oligosaccharides (data not shown) and therefore was not studied in depth. All other enzymes were active on β-1,4 glucan [Carboxymethylcellulose (CMC) and PASC], mixed linked β-1,3/1,4-glucans (barley β-glucan and lichenan), β-1,3 glucan (curdlan), and branched β-1,3 glucans (laminarin). PASC, prepared from Avicel using phosphoric acid, is generally more reactive and homogeneous than Avicel or filter paper (Walseth 1952). CMC is a chemically-modified amorphous cellulose preparation, where some of its hydroxyl groups have been substituted by carboxymethyl groups, making it relatively soluble and more accessible to enzymes (Wood and Bhat, 1988). These experiments confirmed the broad substrate specificity observed for *P. anserina* *Pa*Gluc131A (Lafond et al., 2012). No activity was detected on xyloglucan, polygalacturonic acid, or chitin for any of the enzymes tested. Contrary to the previous report for the *P. anserina* *Pa*Gluc131A (Lafond et al. 2012), we did not detect any enzymatic activity on pustulan (β-1,6 linked glucan) for any of the tested GH131 enzymes. All enzymes were active on β-1,4 linked glucans, with their main products showing a degree of polymerization (DP) ranging from 2 to 4 (Fig. 4-A). A lower activity was detected on PASC, which indicates a preference for soluble or amorphous cellulose substrates. The level of activity per nmol of enzyme was comparable among the GH131 tested (Table 3). All enzymes showed a decreasing activity towards cello-oligosaccharides as chain length decreased. This is consistent with an endo-activity for this group of enzymes. Most of enzymes had a low but detectable activity on purely β-1,3 linked glucan substrates,

which could be attributed partly to the low solubility of such substrates such as curdlan. Only *P. anserina Pa*Gluc131A had high activity on curdlan (Fig. 4-B). We could not detect any activity on the insoluble pachyman, a mostly β-1,3 linked glucan. Barley β-glucan and lichenan are unbranched homopolymers of glucosides linked through β-1,4 linkages, with intermittent β-1,3 linkages, lichenan having a higher proportion of β-1,3 to β-1,4 linkages (Rahar et al. 2011; Meyer and Gürtler 1947; Gorin and Iacomini 1984). Barley β-glucan was generally less digestible compared to lichenan and activities on both polysaccharides produced mostly DP2, DP3 and DP4 cello-oligosaccharides (Fig. 4-C). Larger unidentified peaks were likely mixed linked oligosaccharides (Fig. 4-C, after 22 min of retention time). The *Pycnoporus* GH131 enzymes and the *C. higginsianum Ch*Gluc131B displayed higher activities on lichenan and barley β-glucan than the other tested GH131 enzymes. Regarding oligosaccharides with mixed β-1,4, β-1,3 bonds, the enzymes were active on glucosyl-1,3-β-D-cellotriose (G4A) and glucosyl-1,3-β-D-cellobiose (G3A), which have the β-1,3 bond at the non-reducing end, and released glucose and cellotriose or cellobiose respectively (Fig. 4-D). It seems that the enzymes act on the non-reducing end of the oligomers, cleaving the β-1,3 bond. Overall, GH131 enzymes were able to cleave the β-1,3-glucosidic bonds either on the reducing end of oligomers, releasing glucose, or through endo-action on polymers, releasing mainly β-1,3-oligosaccharides. When both β-1,3 and β-1,4 bonds were present, the main oligosaccharides detected corresponded to cello-oligosaccharides. Laminarin is a low-molecular-weight polysaccharide of algal origin composed of mainly β-1,3-linked glucose units, with β-1,6-linked branched and interstrand glucose residues (Annan et al. 1965). We detected numerous peaks in the chromatograms of GH131-treated laminarin, from which we could identify laminari-biose, -triose and -tetraose. Additional peaks in close proximity to β-1,3-glucooligosaccharides could correspond to small chain oligosaccharides with β-1,6 linkages (Fig. 4-E). This indicates that the branching units can be accommodated by GH131 enzymes for the cleavage of the main chain. The generally higher activity on laminarin than on curdlan (linear β-1,3 glucan) may be related to the higher solubility of laminarin in the conditions used in these assays. In line with this hypothesis, all tested GH131 enzymes were active on the more soluble non-substituted β-1,3-linked laminari-oligosaccharides. In all assays, we detected a range of short laminari-oligosaccharides, rather than glucose, suggesting that the tested GH131

enzymes cleave preferentially β-1,3 bonds through endo-action, while no activity was observed on β-1,6 bonds for any of the tested enzymes.

GH131 can act synergistically with a cellobiohydrolase to degrade cellulose

In order to experimentally demonstrate that GH131 enzymes can act on PCW glucosaccharides, we evaluated the synergy between *P. sanguineus Ps*Gluc131A and a cellobiohydrolase from *Trichoderma reesei* (CBHI, Cel7A) for the enzymatic depolymerisation of cellulose using a complex PCW substrate. Using birch wood as substrate, PsGluc131A released DP2 (cellobiose), DP3 (cellotriose), and DP4 (cellotetraose) oligosaccharides after 24 hours, while CBHI was not able to release any of these oligosaccharides (Fig. 5A). When *Ps*Gluc131A and CBHI were combined, the amount of DP2 oligosaccharides (cellobiose) produced was increased by 3-fold compared to the CBHI alone (Fig. 5). This suggested that *Ps*Gluc131A acts as an endoglucanase to generate shorter chains which were further processed by the cellobiohydrolase (Fig. 5B).

Discussion

GH131 evolution in Fungi: duplications, losses, and Horizontal Gene Transfers (HGT)

Within the extended genome data set we analysed, GH131-coding genes are confined to oomycetes and fungi. They are wide-spread in the fungal kingdom, but are absent from all except one Early Diverging Fungi we analysed and from basal lineages of Basidiomycota (Ustilagomycotina) and Ascomycota (Saccharomycotina, Taphrinomycotina). This distribution of GH131-coding genes strongly differs from the distribution of GH28 pectinases and phytohormone receptors which were probably inherited from a eukaryote ancestor that fungi shared with the green lineage (Streptophytes; Chang et al., 2015; Hérivaux et al., 2015). Phylogenetic reconstruction suggests the HGT of the GH131 progenitor between the common ancestor of Basidiomycota and Ascomycota and the common ancestor of the Peronosporales and Pythiales (Oomycetes), but did not allow the inference of the direction of the HGT. Although GH131 gene loss in all taxa except Fungi and Oomycota cannot be ruled out, the lack of GH131-coding genes in all other Stramenopiles, Alveolates and Rhizaria (the eukaryote super group that includes Oomycetes), and from all other Opisthokonts (the eukaryote super group that includes Fungi) supports our HGT hypothesis. Although the mechanism that allowed exchange of genetic material from Fungi to Oomycetes is still unknown, there are now at least 40 gene families that have been proposed to result from such transfers and it is suggested that these events contributed to the adaptation of Oomycetes to osmotrophy and plant parasitism, specifically in the plant pathogen *Phytophthora* spp. (reviewed in Savory et al. 2015). Among the candidates for HGT are genes coding for PCW degrading enzymes, such as endoglucanases, pectate lyases, polygalacturonases and proteins with carbohydrate-binding modules (Savory et al. 2015). Our findings suggest that GH131 genes could have similarly contributed to the convergent evolution of plant parasitic Fungi and Oomycetes. Our analysis also indicates that the occurrence of a GH131 coding gene in the Early Diverging Fungus *Gonapodya prolifera* could result from a horizontal transfer event between species from Chytridiomycota and the Magnaporthales lineages. *Gonapodya prolifera* is an aquatic fungus that colonizes plant debris (Chang et al., 2015). The order Magnaporthales not only includes devastating pathogens of monocots, but also saprotrophic species associated with grass roots and submerged wood,

suggesting that ancient species from both lineages could have shared a same ecological niche, a pre-requisite for eventual gene transfer.

GH131 occurrence and expression in fungi are correlated with a plant-associated lifestyle

GH131 paralogs were detected in the genomes of a wide range of fungi that feed on plant tissues. The increase in GH131 gene numbers in plant saprobic, pathogenic and symbiotic fungal species suggests they could play an important role in PCW modifications during plant-tissue colonisation. Our survey of transcriptomics data revealed that at least one GH131 gene is up-regulated during biotrophic and/or necrotrophic stages of plant colonisation/infection. A wider survey of available transcriptomics data for the ectomycorrhizal fungi *Hebeloma cylindrosporum*, *Piloderma croeus* and *Cenococcum geophilum* (Kohler et al., 2015; Peter et al., 2016) confirmed this trend. Some exceptions however were found in *Suillus luteus* in which the single GH131 gene was not found up-regulated and in *Amanita muscaria* which lacks GH131 genes (Kohler et al., 2015). GH131 genes are expressed at all infection stages in symbiotic and plant pathogenic fungi. In particular, some GH131 genes are expressed during the biotrophic stage of plant pathogenic fungi that requires minimal PCW modifications in order to maintain plant cell viability. This expression pattern suggests that GH131 enzymes cause only moderate and targeted disruption of PCW polymers.

GH131 are β-glucanases with broad substrate specificity involved in PCW deconstruction

A striking feature of *Pa*Glu131A from *P. anserina* was its broad specificity towards β-1,3, β-1,4 and β-1,6 glucosidic linkages (Lafond et al. 2012), rendering it active towards both plant- and fungal-cell-wall polysaccharides. This peculiarity was supported by the crystal structure of the enzyme that revealed a substrate binding site that could potentially accommodate a wide range of β-glucan isomers (Jiang et al. 2013; Miyazaki et al. 2013). For the seven additional GH131 enzymes studied here, we confirmed their broad specificity towards β-1,3 and β-1,4-glucan linkages, as well as their ability to accommodate

in their active site β-1,3; β-1,4 and (β-1,3; β-1,6) mixed linkages. Due to their endo-β-1,4-glucanase activity, GH131 enzymes can act on cellulose, which is a major structural component of the barrier that fungi need to loosen during plant-tissue colonisation. Our results suggest that GH131 enzymes may contribute to loosening cellulose microfibrils by targeting amorphous cellulose regions. As the cell wall of oomycetes contains cellulose (Bartnicki-Garcia, 1968), activity towards β-1,4 glucosidic bonds could have a dual role in oomycetes, contributing towards the hydrolysis of the PCW and the restructuring of the cell wall of oomycetes during growth. While we have identified GH131 genes only in Peronosporales and Pythiales, which are dominated by phytopathogenic oomycetes, transcriptome data for *P. sojae* suggest that GH131 are expressed in both free mycelia and 3 h after infection of soybean, but not in the zoospores nor the germinated cysts, where plant colonisation is initiated (Ye et al., 2011). In this light, a broader role in the development of the mycelium cell wall in and out of the host seems plausible. Besides the role of GH131 in cellulose deconstruction, additional substrate specificities suggest further roles in PCW remodelling or deconstruction. Mixed linked β-1,3/1,4-glucans are abundant in the primary cell walls of Poaceae (syn. Gramineae, including barley, maize, millet, rice, and wheat) and other families of the order Poales (Smith and Harris 1999), in which they locally adsorb to cellulose (Kiemle et al. 2014). In *Z. tritici* and *C. graminicola,* both pathogenic fungi that infest Poaceae, GH131-coding genes are upregulated during the necrotrophic and/or the biotrophic phase of the interaction with the plant. Thus, GH131 enzymes may contribute to PCW remodelling or breakdown by cleaving hemicellulosic β-1,3/1,4 bonds or facilitating access of other enzymes to cellulose.

GH131-coding genes are co-expressed with genes of other PCW-degrading enzymes during plant tissue colonisation

GH131 enzymes may participate in cellulose breakdown in association with complementary enzymes that are also active on cellulose and can be expected to be co-regulated (Ilmen et al. 1997). For example, in *L. bicolor*, three beta-1,4-endoglucanases (GH12 and GH5_5) and three AA9 LPMOs are up-regulated during the interaction and the GH5_5 endoglucanase was identified as a key factor for

establishment of the ectomycorrhiza (Veneault-Fourrey et al., 2014; Zhang et al., 2018). In *Z. tritici*, genes coding for a GH7 cellobiohydrolase, a GH12 and two GH5_5 endoglucanases were up-regulated during the necrotrophic phase and could participate in the cellulose breakdown together with the ZtGluc131A-coding gene selected here (Rudd et al. 2015; Palma-Guerrero et al. 2016). In *C. graminicola*, a broad range of genes coding for cellulose-active enzymes were significantly up-regulated during the necrotrophic phase as compared to the biotrophic phase or the formation of the penetration appressorium, including three GH5, two GH6, three GH7, one GH12, one GH45 and nine AA9 LPMOs, a family of lytic oxidases mainly active on cellulose (O'Connell et al., 2012). In *C. higginsianum,* genes coding for two GH5, one GH6, two GH7, and two GH12 were upregulated during that phase compared to *in vitro* growth (O'Connell et al., 2012). In a previous study on the response of the saprotrophic fungi *P. sanguineus, P. coccineus*, and *P. cinnabarinus* to growth on lignocellulosic and woody substrates (Miyauchi et al. 2016), GH131 enzymes were shown to be co-secreted with GH6 and GH7 cellobiohydrolases, GH5_5 and GH45 endoglucanases, and AA9s. Co-secretion of GH131 enzymes with other cellulose-acting enzymes suggests that despite their relatively low specific activity, these enzymes could either facilitate access to the substrate for other enzymes or act in synergy with these enzymes to facilitate cellulose degradation. Here we demonstrated synergy between PsGluc131A and a GH7 cellobiohydrolase on a substrate that resembles the natural substrates of *P. sanguineus*. These findings suggest that GH131 alone creates moderate alterations of PCW, and that it enhances the more extensive PCW breakdown by complementary enzymes produced during saprotrophy or necrotrophy.

GH131 activity on plant and fungal cell wall beta-1,3 glucans

All tested GH131 enzymes were also active on β-1,3-linked glucans. Callose is a linear β-(1→3)-D-Glcp homo-polymer deposited as a highly localised plant defence mechanism at the sites of fungal penetration which acts as both a physical and chemical barrier to pathogens (Luna et al. 2011). Fungi that colonise living plant tissues may utilise GH131 enzymes to bypass the callose barrier. However,

studying the depolymerisation of non-soluble polysaccharides is a challenging task and new technologies such as QCM-D (Goacher et al., 2014) still need to be optimized to help resolve whether enzymes that produce scattered cleavages on long polymers can act on such substrates. A β-(1,3) glucosidic backbone with β-1,6 branches can be found in the fungal cell-wall, linked to chitin through β-1,4 bonds (Latgé JP 2007) and in the cell wall of oomycetes (Bartnicki-Garcia, 1968). The ability of all tested GH131 to accommodate (β-1,3; β-1,6) bonds from laminarin suggest that GH131 enzymes could function in remodelling the fungal cell wall during plant colonisation and/or nutrient extraction. This hypothesis is supported by strong transcriptional up-regulation of GH16 and GH30 beta-1,6-glucanase genes during plant tissue colonization in the fungi analyzed here (O'Connell et al. 2012; Gan et al. 2013; Veneault-Fourrey et al. 2014; Miyauchi et al. 2016) and the extensive fungal cell wall rearrangements generally observed during plant-fungus interactions (Balestrani et al., 2014; Geoghegan et al., 2017). This activity could also contribute to the virulence arsenal of certain mycoparasitic fungi which involves β -(1,4)-, β -(1,3)- and β -(1,6)-glucanases, and proteases (Benítez et al., 2004).

Materials and Methods

Distribution of GH131-coding genes

We searched for GH131-coding genes in all finished genomes available on Genbank (last accessed on July 02, 2017) and in fungal genomes publicly available on the JGI Mycocosm portal (https://genome.jgi.doe.gov/programs/fungi/index.jsf). For each analysed genome, all predicted proteins were searched for GH131 modules using blastp. HMMer 3 (Finn et al. 2011) was used to query against GH131 custom-made hidden Markov model (HMM) profiles. All identified proteins were manually curated. Absence of GH131-coding genes from the respective genomes was verified with tblastn, with the exception of *Fusarium oxysporum*, for which one GH131 was identified in this way. Correlations between the distribution of GH131-coding genes and fungal lifestyles were analysed using generalised least squares in R using the gls function from package nlme, using Martin's correlation structure from package ape (Paradis et al. 2004). All species were grouped under four lifestyles, plant

pathogens (PP), saprotrophs (S), symbionts (SYM; including mycorrhizal species and endophytes), and non-plant-associated species (including all other lifestyles).

Phylogenetic analysis

The sequences corresponding to the catalytic modules (*viz.* after removal of the CBM1 domains where existing) were manually refined from the predicted protein models and aligned with Clustal Omega (Sievers et al. 2011), using default parameters. After alignment, the sequences were further screened for mis-assigned introns, and missing N- or C-termini. Phylogenetic relationships were inferred with MrBayes 3.2 (Ronquist et al. 2012) at the CIPRES Science Gateway (Miller et al. 2011) and the WAG model (Whelan and Goldman, 2001). Four Markov cold chains with three hot chains each ran for 35.8 million generations, with sampling every 1000 generations. Bayesian inference was conducted under a mixed substitution model (aamodel=mixed) with estimated proportion of invariable sites, and estimated variation of the remaining sites based on a gamma distribution approximated using five categories (lset rates=invgamma). The prior probability distribution on branch lengths was set to unconstrained:exponential (10.0), the prior of the state frequencies to dirichlet(1.0), the temperature to 0.06, and the prior for the proportion of invariable sites was kept to its default setting (pinvarpr=uniform(0.0,1.0)). At the end of the run, although the average standard deviation of split frequencies for the four different runs had only reached 0.02, the potential scale reduction factor (PSRF) had reached 1.0 for all parameters (tree length, alpha, pinvar). Sufficient sampling was verified with the Estimated Sample Size and verified with Tracer v1.6 (Rambaut and Drummond 2013). The first 8960 (25%) of the sampled trees from each run were discarded as the burn-in. The 50% majority consensus tree resulted from 32,256 trees from each run, with the nodes indicating the posterior probability. The tree was viewed with FigTree (Rambaut 2016). The harmonic mean of likelihood was estimated as -52627. The inference of the cluster containing the early diverging fungus *G. prolifera* was verified by constructing phylogenetic trees of all the sequences with Neighbour Joining and Maximum Parsimony

453 using MEGA 6.06 with default settings, partial and pairwise deletion, and 100 bootstrap replications
454 (Tamura et al. 2013; Felsenstein, 1985).

455 For the species tree-gene tree reconciliation study, the midpoint-rooted protein tree was used as the gene
456 tree. The species tree was generated from the proteome analysis with Orthofinder (Emms and Kelly
457 2015), using DIAMOND for sequence search (Buchfink et al. 2015), Clustal Omega for the alignment
458 (Sievers et al. 2011), and FastTree for the tree generation (Price et al. 2009). The resulted rooted species
459 tree was rerooted at the branching point between Oomycetes and Fungi (Fig. 1). Prior to reconciliation,
460 branch lengths were removed and the following species were manually added, according to Burki
461 (2014): *Trypanosoma brucei-gambiense, Leishmania infantum, Bathycoccus prasinos, Arabidopsis*
462 *thaliana, Toxoplasma gondii, Plasmodium malariae, Saprolegnia parasitica, Schizochytrium*
463 *aggregatum, Bigelowiella natans, Dictyostelium discoideum.* The set of costs for gene duplications,
464 transfers, and losses that gave feasible reconciliation solutions was manually investigated using Notung
465 2.9 (Durand et al. 2006). The survey of the event cost space was performed with xscape (Libeskind-
466 Hadas et al. 2014), using a range of costs for transfers between 5.8 and 8, and losses cost between 0.2
467 and 0.9. We investigated the events that were common between transfer cost 5.8 and 6.0 and loss cost
468 0.3 and 0.5, as well as transfer costs 7.8-8.0 and loss costs 0.1-0.5, allowing the coverage of none to up
469 to 12 transfers. Finally, the gene tree was rerooted, using Notung 2.9 (Durand et al. 2006), at the
470 branching point between the fungal and oomycetes GH131 clades. Notung 2.9 was also used to infer
471 the number of GH131 genes in the internal nodes of the species tree (Fig. 1) by reconciling the genes
472 and species trees with a loss cost of 0.5, a duplication cost of 1, and transfer costs between 5.8 and 9
473 with 0.2 intervals. The average gene copy numbers as deduced from reconciliations allowing 1 to 12
474 transfer events are presented on each branch.

475

476 **Transcriptome data analysis**

477 Transcriptome data for the GH131-coding genes were extracted from published studies. We compared
478 the transcription profiles in the following conditions: (i) Biotrophic vs. necrotrophic stages of infection

for *C. higginsianum* on *Arabidopsis thaliana* and *C. graminicol*a on maize (O'Connell et al. 2012); (ii) Asymptomatic vs. necrotrophic stages of infection for *Z. tritici* on wheat leaves (Rudd et al. 2015; Palma-Guerrero et al. 2016); (iii) free-living mycelium vs. ectomycorrhizal stage for *L. bicolor* California poplar (*Populus trichocarpa*; Veneault-Fourrey et al. 2014); (iv) saprotrophic growth on dead plant tissues, such as wheat straw, pine wood and aspen wood vs. maltose as a carbon source for *P. sanguineus*, *P. cinnabarinus*, and *P. coccineus* (Miyauchi et al. 2016).

Enzyme cloning, production and purification

The coding sequences of the selected GH131s were optimised for *Pichia pastoris*, synthesized and cloned into the pPICZαA plasmid by Genscript (NJ, U.S.A), so that open reading frames were in frame with the α-signal factor and the His6 epitope at the C-terminus, while preserving the N-terminus of the protein. The plasmid was then linearised with PmeI (Thermo Fisher Scientific) and inserted in *P. pastoris* X-33 with electroporation, using a Micropulser Electroporator (Bio-Rad, CA, U.S.A) and according to the manufacturer's instructions. The transformants were selected in YPD medium (Glucose, 20 g L^{-1}, yeast extract, 10 g L^{-1}, bacteriological peptone, 20 g L^{-1}, Agar, 15 g L^{-1}) with Zeocin (Thermo Fisher Scientific) concentrations of 100 and 250 µg mL^{-1}. The production was performed according to standard methods (Thermo Fisher Scientific) using Buffered Minimal Glycerol Medium for growth and Buffered Minimal Methanol Medium for induction supplemented with 3% methanol every day of induction. Production was assayed at two different temperatures (20 °C and 27 °C) and two different culture scales (deep-well and flask cultures) as described in Haon et al., (2015), and was evaluated with SDS-PAGE. Purification of the enzymes was performed using either the Hisprep FF 16/10 column (GE Healthcare) on the Äkta Purifier and Äkta Express according to the instructions of the manufacturer or using our in-house Tecan robotic system, as previously described (Haon et al. 2015).

Enzymatic assays

All enzymatic assays were performed in 50 mM Acetate buffer pH5 at 50 °C for 24 h. The concentration of the substrate was 1 % for polysaccharides and 100 µM for oligosaccharides. Carboxymethylcellulose, low viscosity, and laminarin, were purchased from Sigma-Aldrich (St. Louis, MO); cello-oligosaccharides with a degree of polymerisation (DP) from two (DP2) to six (DP6) glucose units, laminari-oligosaccharides from two to six glucose units, barley β-glucan, lichenan, curdlan, pachyman, mixed linkage oligosaccharides (β-glucosyl-(1→3)-β-glucosyl-(1→4)-β-glucosyl-(1→4)-glucose (G4A), β-glucosyl-(1→4)-β-glucosyl-(1→4)-β-glucosyl-(1→3)-glucose (G4B), β-glucosyl-(1→4)-β-glucosyl-(1→3)-β-glucosyl-(1→4)-glucose (G4C), β-glucosyl-(1→3)-β-glucosyl-(1→4)-glucose (G3A), β-glucosyl-(1→4)-β-glucosyl-(1→3)-glucose (G3B)), polygalacturonic acid, and gentiobiose were purchased from Megazyme (Wicklow, Ireland). Pustulan was purchased from Elicityl SA (Crolles, France). PASC was prepared from Avicel PH-101 (Sigma-Aldrich, St. Louis, MO) according to Wood et al. (1988). Birch fibres were provided by S. Tapin (CTP, Grenoble, France).

Reactions were stopped by boiling for 15 min, the reaction mixtures were centrifuged, and the soluble products were analysed with High Performance Anion Exchange Chromatography coupled with Pulsed Amperometric Detection (HPAEC-PAD). A CarboPac PA1 column (4 × 250 mm; Dionex, Thermo Scientific, Waltham, MA, USA), preceded by a Carbopac PA1 guard column (4 × 50 mm, Dionex) was used for the separation. The column was maintained at 30 °C and pre-equilibrated for 8 min with 130 mM NaOH. Ten µl were injected and eluted with a rate of 1 mL min^{-1}. A linear gradient of sodium acetate from 0 to 195 mM in 25 min was applied, followed by isocratic elution for 5 min. The products of the enzymatic reaction were identified and quantified based on the respective standards (Megazyme, Wicklow, Ireland).

Acknowledgements

This work was supported by the French National Agency for Research (ANR-11-IDEX-0001-02, ANR-14-CE06-0020-01, and ANR-13-BIME-0002). The authors would like to thank Nicolas Lopez Ferreira from IFPEN for the purification of CBHI from *T. reesei*. GEA would like to thank the AgreenSkills

fellowship programme, which has received funding from the EU's Seventh Framework Programme (FP7-26719). The work conducted by the U.S. Department of Energy Joint Genome Institute (JGI), a DOE Office of Science User Facility, was supported by the Office of Science of the U.S. Department of Energy under Contract No. DE-AC02-05CH11231. Authors have no conflict of interest.

Author contribution

JGB and MNR designed the research with support from MHL, ROC, BH and FM. GEA, MH, CC, NL, MHL, BH, and AK conducted the research. IVG, RR provided genomic information. GEA, MNR and MHL wrote the manuscript.

References

Annan WD, Hirst E, Manners DJ. 1965. 162. The constitution of laminarin. Part V. The location of 1,6-glucosidic linkages. Journal of the Chemical Society (Resumed):885.

Baldauf SL, Roger AJ, Wenk-Siefert I, Doolittle WF. 2000. A kingdom-level phylogeny of eukaryotes based on combined protein data. Science. 290:972-977.

Balestrini R, Bonfante P. 2014. Cell wall remodelling in mycorrhizal symbiosis: a way towards biotrophism. Front Plant Sci. 5:237.

Bartnicki-Garcia S. 1968. Cell wall chemistry, morphogenesis, and taxonomy of fungi. Annu Rev Microbiol. 22:87–108.

Beckham GT, Matthews JF, Peters B, Bomble YJ, Himmel ME, Crowley MF. 2011. Molecular-level origins of biomass recalcitrance: decrystallization free energies for four common cellulose polymorphs. J Phys Chem B. 115:4118-27.

Benítez T, Rincón AM, Limón MC, Codón AC. 2004. Biocontrol mechanisms of *Trichoderma* strains. Int Microbiol. 7(4):249-60.

Berbee ML, James TY, Strullu-Derrien C. 2017. Early diverging fungi: diversity and impact at the dawn of terrestrial life. Annu Rev Microbiol. 71:41-60.

Berrin JG, Rosso MN, Abou Hachem M. 2017. Fungal secretomics to probe the biological functions of lytic polysaccharide monooxygenases. Carbohydr Res. 448:155-160.

Buchfink B., Xie C., Huson D. 2015. "Fast and sensitive protein alignment using DIAMOND", Nature Methods 12:59-60.

560 Burki, 2014. The Eukaryotic tree of life from a global phylogenomic perspective. Cold Spring Harb
561 Perspect Biol, 6:a016147.

562 Cavalier-Smith T, Chao EE-Y. 2006. Phylogeny and megasystematics of phagotrophic heterokonts
563 (Kingdom Chromista). J. Mol. Evol. 62:388-420.

564 Chang Y, Wang S, Sekimoto S, Aerts AL, Choi C, Clum A, LaButti KM, Lindquist EA, Yee Ngan C,
565 Ohm RA et al. 2015. Phylogenomic analyses indicate that early fungi evolved digesting cell walls of
566 algal ancestors of land plants. Genome Biol Evol 7:1590-1601.

567 Cosgrove DJ. 2005. Growth of the plant cell wall. Nat Rev Mol Cell Biol. 6(11):850-861.

568 Couturier M, Ladeveze S, Sulzenbacher G, Ciano L, Fanuel M, Moreau C, Villares A, Cathala B,
569 Chaspoul F, Fradsen KE, et al. 2018. Lytic xylan oxidases from wood-decay fungi unlock biomass
570 degradation. Nat Chem Biol, 14:306-310.

571 Duncan KE, Howard RJ. 2000. Cytological analysis of wheat infection by the leaf blotch pathogen
572 Mycosphaerella graminicola. Mycol Res. 104:1074-1082.

573 Durand D., Halldorsson B. V., Vernot B. 2006. A hybrid micro-macroevolutionary approach to gene
574 tree reconstruction. J Comput Biol, 13(2):320-335.

575 Emms DM, Kelly S. 2015. OrthoFinder: solving fundamental biases in whole genome comparisons
576 dramatically improves orthogroup inference accuracy. Genome Biol. 16:157.

577 Felsenstein J. 1985. Confidence limits on phylogenies: an approach using the bootstrap. Evolution
578 39:783-791.

579 Finn R, Clements J, Eddy S. 2011. Hmmer web server: Interactive sequence similarity searching.
580 Nucleic Acids Res 39:W29-37

581 Gan P, Ikeda K, Irieda H, Narusaka M, O'Connell RJ, Narusaka Y, Takano Y, Kubo Y, Shirasu K.
582 2013. Comparative genomic and transcriptomic analyses reveal the hemibiotrophic stage shift of
583 *Colletotrichum* fungi. New Phytol. 197:1236-1249.

584 Geoghegan I, Steinberg G, Gurr S. The role of the fungal cell wall in the infection of plants. 2017.
585 Trends Microbiol. 25(12):957-967.

586 Goacher RE, Selig MJ, Master ER. 2014. Advancing lignocellulose bioconversion through direct
587 assessment of enzyme action on insoluble substrates. Curr Opin Biotechnol. 27:123-133.

588 Goodwin SB, M'Barek S B, Dhillon B, Wittenberg AH, Crane CF, Hane JK, Foster AJ, Van der Lee
589 TA, Grimwood J, Aerts A et al. 2011. Finished genome of the fungal wheat pathogen *Mycosphaerella*
590 *graminicola* reveals dispensome structure, chromosome plasticity, and stealth pathogenesis. PLoS
591 Genetics 7:e1002070.

592 Gorin PAJ, Iacomini M. 1984. Polysaccharides of the lichens *Cetraria islandica* and *Ramalina usnea*.
593 Carbohydr Res 128:119-132.

594 Gupta VK, Kubicek CP, Berrin JG, Wilson DW, Couturier M, Berlin A, Filho EX, Ezeji T. 2016. Fungal
595 enzymes for bio-products from sustainable and waste biomass. Trends BiochemSci 41:633-645.

Haon M, Grisel S, Navarro D, Gruet A, Berrin JG, Bignon C. 2015. Recombinant protein production facility for fungal biomass-degrading enzymes using the yeast *Pichia pastoris*. Front Microbiol 6:1002.

Heckman DS, Geiser D M, Eidell BR, Stauffer RL, Kardos NL, Hedges SB. 2001. Molecular evidence for the early colonization of land by fungi and plants. Science. 293 (5532):1129-1133.

Hérivaux A, Dugé de Bernonville T, Roux C, Clastre M, Courdavault V, Gastebois A, Bouchara J-P, James TY, Latgé J-P, Martin F and Papon N. 2017. The identification of phytohormone receptor homologs in early diverging fungi suggests a role for plant sensing in land colonization by fungi. mBio. 8(1).

Ilmen M, Saloheimo A, Onnela ML, Penttila ME. 1997. Regulation of cellulase gene expression in the filamentous fungus *Trichoderma reesei*. Appl Environ Microbiol 63:1298-1306.

Jiang T, Chan HC, Huang CH, Ko TP, Huang TY, Liu JR, Guo RT. 2013. Substrate binding to a GH131 beta-glucanase catalytic domain from *Podospora anserina*. Biochem Biophys Res Commun 438:193-197.

Kiemle SN, Zhang X, Esker AR, Toriz G, Gatenholm P, Cosgrove DJ. 2014. Role of (1,3)(1,4)-β-glucan in cell walls: Interaction with cellulose. Biomacromolecules 15:1727-1736.

Kohler A, Kuo A, Nagy LG, Morin E, Barry KW, Buscot F, Canback B, Choi C, Cichocki N, Clum A et al. 2015. Convergent losses of decay mechanisms and rapid turnover of symbiosis genes in mycorrhizal mutualists. Nat Genet 47:410-415.

Lafond M, Navarro D, Haon M, Couturier M, Berrin JG. 2012. Characterization of a broad-specificity beta-glucanase acting on beta-(1,3)-, beta-(1,4)-, and beta-(1,6)-glucans that defines a new glycoside hydrolase family. Appl Environ Microbiol 78:8540-8546.

Latgé JP. 1999. *Aspergillus fumigatus* and aspergillosis. Clin Microbiol Rev. 12(2):310-50.

Latge JP. 2007. The cell wall: a carbohydrate armour for the fungal cell. Mol Microbiol 66:279-290.

Leroux O, Sørensen I, Marcus SE, Viane RL, Willats WG, Knox JP. 2015. Antibody-based screening of cell wall matrix glycans in ferns reveals taxon, tissue and cell-type specific distribution patterns. BMC Plant Biol 15:56

Levasseur A, Lomascolo A, Chabrol O, Ruiz-Duenas FJ, Boukhris-Uzan E, Piumi F, Kues U, Ram AF, Murat C, Haon M et al. 2014. The genome of the white-rot fungus *Pycnoporus cinnabarinus*: a basidiomycete model with a versatile arsenal for lignocellulosic biomass breakdown. BMC Genomics 15:486.

Libeskind-Hadas R., Wu Y-C., Bansal M.S., and Kellis M. 2014. Pareto-Optimal Phylogenetic Tree Reconciliation. Bioinformatics, Proceedings of ISMB 2014 30:i87–i95.

Luna E, Pastor V, Robert J, Flors V, Mauch-Mani B, Ton J. 2011. Callose deposition: a multifaceted plant defense response. Mol Plant-Microbe Interact 24:183-193.

Lutzoni F., Nowak M.D., Alfaro M.E., Reeb V., Miadlikowska J., Krug M., Arnold A.E., Lewis L.A., Swofford D.L., Hibbett D., Hilu K., James T.Y., Quandt D., Magallón S. 2018. Contemporaneous radiations of fungi and plants linked to symbiosis. Nat Commun. 9:5451.

Martin F, Aerts A, Ahren D, Brun A, Danchin EGJ, Duchaussoy F, Gibon J, Kohler A, Lindquist E, Pereda V et al. 2008. The genome of *Laccaria bicolor* provides insights into mycorrhizal symbiosis. Nature 452:88-92.

Meyer KH, Gürtler P. 1947. Recherches sur l'amidon. XXXI. La constitution de la lichénine. Helvetica Chimica Acta 30:751-761.

Miller MA, Pfeiffer W, Schwartz T. 2011. The CIPRES Science Gateway: A community resource for phylogenetic analyses. In: Proceedings of the 2011 TeraGrid Conference: Extreme Digital Discovery. TG '11. New York, NY, USA: ACM. p. 41:1--41:8. doi.acm.org/10.1145/2016741.2016785.

Miyauchi S, Navarro D, Grigoriev IV, Lipzen A, Riley R, Chevret D, Grisel S, Berrin JG, Henrissat B, Rosso MN. 2016. Visual comparative omics of fungi for plant biomass deconstruction. Front Microbiol 7:1335.

Miyazaki T, Yoshida M, Tamura M, Tanaka Y, Umezawa K, Nishikawa A, Tonozuka T. 2013. Crystal structure of the N-terminal domain of a glycoside hydrolase family 131 protein from *Coprinopsis cinerea*. FEBS Lett 587:2193-2198.

Munch S, Lingner U, Floss DS, Ludwig N, Sauer N, Deising HB. 2008. The hemibiotrophic lifestyle of *Colletotrichum* species. J Plant Physiol 165:41-51.

O'Connell R, Herbert C, Sreenivasaprasad S, Khatib M, Esquerre-Tugaye MT, Dumas B. 2004. A novel *Arabidopsis*-*Colletotrichum* pathosystem for the molecular dissection of plant-fungal interactions. Mol Plant-Microbe Interact 17:272-282.

O'Connell RJ, Thon MR, Hacquard S, Amyotte SG, Kleemann J, Torres MF, Damm U, Buiate EA, Epstein L, Alkan N et al. 2012. Lifestyle transitions in plant pathogenic *Colletotrichum* fungi deciphered by genome and transcriptome analyses. Nature Genet 44:1060-1065.

Palma-Guerrero J, Torriani SFF, Zala M, Carter D, Courbot M, Rudd JJ, McDonald BA, Croll D. 2016. Comparative transcriptomic analyses of *Zymoseptoria tritici* strains show complex lifestyle transitions and intraspecific variability in transcription profiles. Mol Plant Pathol17:845–859.

Paradis E., Claude J. & Strimmer K. 2004. APE: analyses of phylogenetics and evolution in R language. Bioinformatics 20:289-290.

Perfect SE, Hughes HB, O'Connell RJ, Green JR. 1999. *Colletotrichum*: A model genus for studies on pathology and fungal-plant interactions. Fungal Genet Biol 27:186-198.

Peter M, Kohler A, Ohm RA, Kuo A, Krützmann J, Morin E, Arend M, Barry KW, Binder M, Choi C, Clum A, Copeland A, Grisel N, Haridas S, Kipfer T, LaButti K, Lindquist E, Lipzen A, Maire R, Meier B, Mihaltcheva S, Molinier V, Murat C, Pöggeler S, Quandt CA, Sperisen C, Tritt A, Tisserant E, Crous PW, Henrissat B, Nehls U, Egli S, Spatafora JW, Grigoriev IV, Martin FM. 2016. Ectomycorrhizal ecology is imprinted in the genome of the dominant symbiotic fungus *Cenococcum geophilum*. Nat Commun. 7:12662.

Price MN., Dehal PS, Arkin AP. 2009. FastTree: Computing Large Minimum-Evolution Trees with Profiles instead of a Distance Matrix. Mol Biol Evol 26:1641-1650.

Rahar S, Swami G, Nagpal N, Nagpal MA, Singh GS. 2011. Preparation, characterization, and biological properties of beta-glucans. J Adv Pharm Tech Res 2:94-103.

672 Rambaut A. 2016. FigTree v1.4.3. Mol. Evol. phylogenetics Epidemiol. Available from:
673 http://tree.bio.ed.ac.uk/software/figtree/

674 Rambaut A, Drummond AJ. 2013. Tracer v1.6. Available from http//tree.bio.ed.ac.uk/software/tracer/.

675 Ritter S. 2008. Lignocellulose: A Complex Biomaterial. Chemical & Engineering News 86:15.

676 Ronquist F, Teslenko M, van der Mark P, Ayres DL, Darling A, Hohna S, Larget B, Liu L, Suchard
677 MA, Huelsenbeck JP. 2012. MrBayes 3.2: efficient Bayesian phylogenetic inference and model choice
678 across a large model space. Systematic Biology 61:539-542.

679 Rudd JJ, Kanyuka K, Hassani-Pak K, Derbyshire M, Andongabo A, Devonshire J, Lysenko A, Saqi M,
680 Desai NM, Powers SJ et al. 2015. Transcriptome and metabolite profiling of the infection cycle of
681 *Zymoseptoria tritici* on wheat reveals a biphasic interaction with plant immunity involving differential
682 pathogen chromosomal contributions and a variation on the hemibiotrophic lifestyle definition. Plant
683 Physiol 167:1158–1185.

684 Savory F, Leonard G, Richards TA. 2015. The role of horizontal gene transfer in the evolution of the
685 Oomycetes. PLoS Pathog 11(5): e1004805.

686 Sievers F, Wilm A, Dineen D, Gibson TJ, Karplus K, Li W, Lopez R, McWilliam H, Remmert M,
687 Söding J et al. 2011. Fast, scalable generation of high-quality protein multiple sequence alignments
688 using Clustal Omega. Molecular Systems Biology [Internet] 7:539. Available from:
689 http://europepmc.org/articles/PMC3261699

690 Smith BG, Harris PJ. 1999. The polysaccharide composition of Poales cell walls. Biochem Syst Ecol
691 27:33-53.

692 Soares FEF, Sufiate BL, J de Queiroz JH, 2018. Nematophagous fungi: Far beyond the endoparasite,
693 predator and ovicidal groups. Agriculture and Natural Resources 52(1):1-8.

694 Tamura K, Stecher G, Peterson D, Filipski A, Kumar S. 2013. MEGA6: Molecular Evolutionary
695 Genetics Analysis version 6.0. Mol Biol Evol 30:2725-2729.

696 Veneault-Fourrey C, Martin F. 2011. Mutualistic interactions on a knife-edge between saprotrophy and
697 pathogenesis. Curr Opin Plant Biol 14:444-450.

698 Veneault-Fourrey C, Commun C, Kohler A, Morin E, Balestrini R, Plett J, Danchin E, Coutinho P,
699 Wiebenga A, de Vries RP et al. 2014. Genomic and transcriptomic analysis of *Laccaria bicolor*
700 CAZome reveals insights into polysaccharides remodelling during symbiosis establishment. Fung
701 Genet Biol 72:168-181.

702 de Vries S., de Vries J., von Dahlen J.K., Gould S.B., Archibald J.M., Rose L.E., Slamovits C.H.. 2018.
703 On plant defense signaling networks and early land plant evolution. Commun Integr Biol. 11(3): 1–14.

704 Walseth CS. 1952. Occurence of cellulases in enzyme preparations from microorganisms. Tappi
705 35:228–233.

706 Whelan S, Goldman N. 2001. A general empirical model of protein evolution derived from multiple
707 protein families using a maximum-likelihood approach. Mol Biol Evol 18:691-699.

Wood TM. Preparation of crystalline, amorphous, and dyed cellulase substrates. Methods enzymol. Elsevier. 1988:19–25.

Wood TM, Bhat KMBT-M in E. 1988. Methods for measuring cellulase activities. In: Biomass Part A: Cellulose and Hemicellulose. Vol. 160. Academic Press. p. 87-112.

Ye W, Wang X, Tao K, Lu Y, Dai T, Dong S, Dou D, Gijzen M, Wang Y. 2011. Digital gene expression profiling of the *Phytophthora sojae* transcriptome. Mol. Plant-Microbe Interact. 24:1530–1539.

Zhang F, Anasontzis GE, Labourel A, Champion C, Haon M, Kemppainen M, Commun C, Deveau A, Pardo A, Veneault-Fourrey C, Kohler A, Rosso MN, Henrissat B, Berrin JG, Martin F. 2018. The ectomycorrhizal basidiomycete *Laccaria bicolor* releases a secreted β-1,4 endoglucanase that plays a key role in symbiosis development. New Phytol. 220(4):1309-1321.

Zhao Z, Liu H, Wang C, Xu JR. 2013. Comparative analysis of fungal genomes reveals different plant cell wall degrading capacity in fungi. BMC Genomics 14:274.

720 *Table 1: Fungal lifestyle and number of GH131-coding genes in the genome*

Microorganism	Lifestyle	Number of GH131
C. higginsianum	Hemibiotrophic	8
C. graminicola	Hemibiotrophic	7
Z. tritici	Hemibiotrophic	1
L. bicolor	Ectomycorrhizal	1
P. sanguineus	Saprotrophic	3
P. cinnabarinus	Saprotrophic	3
P. coccineus	Saprotrophic	3

721

722 *Table 2: Relative transcription levels of the GH131-coding genes, between free-living mycelia and*

723 *mycelia colonising their respective plant hosts/substrates.*

Enzyme	Transcript/ Protein ID	Biotrophy, Symbiosis, or Asymptomatic colonisation	Necrotrophy or Saprotrophy	References
LbGluc131A	704573	116[a]	-	Martin et al. 2008; Veneault-Fourrey et al. 2014
ChGluc131A	CH063_00647	98.6[b]	271[c]	O'Connell et al. 2012; Gan et al. 2013
ChGluc131B	CH063_03177	38[b]	0.1[c]	O'Connell et al. 2012; Gan et al. 2013
CgGluc131A	GLRG_10695	5.8[d]	6.7[e]	O'Connell et al. 2012; Gan et al. 2013
PsGluc131A	571793	-	9.6[f]	Miyauchi et al. 2016
PsGluc131B	1756265	-	10.9[f]	Miyauchi et al. 2016
ZtGluc131A	27161	56[g]	27[h]	Rudd et al. 2015 ; Palma-Guerrero et al. 2016

724

725 [a]Ratio of transcription level after 2 weeks of ectomycorrhizae formation on California poplar
726 (*Populus trichocarpa*), to free living mycelium.
727 [b]Ratio of transcription level during the *C. higginsianum* biotrophic phase on *Arabidopsis*
728 *thaliana* to *in vitro* appressoria.
729 [c]Ratio of transcription level during the *C. higginsianum* necrotrophic phase on *Arabidopsis*
730 *thaliana* to *in vitro* appressoria.
731 [d]Ratio of transcription level during the *C. graminicola* biotrophic phase on maize (*Zea mays*)
732 to *in planta* appressoria.
733 [e]Ratio of transcription level during the *C. graminicola* necrotrophic phase on maize (*Zea*
734 *mays*) to *in planta* appressoria.
735 [f]Ratio of the transcription level when *P. sanguineus* was grown on Aspen (*Populus*
736 *grandidentata*), to the respective values when grown on maltose.
737 [g]Ratio of transcription level at 9 days after inoculation on wheat leaves to those in free living
738 mycelium.
739 [h]Ratio of transcription level at 21 days after inoculation on wheat leaves to those in free living
740 mycelium.

Table 3: Activities of the selected GH131 enzymes after incubation for 24 h at 50 °C on different substrates. The activity is represented as the sum of di-, tri-, tetra-, penta-, hexa-saccharides (in nmol) per nmol of enzyme.

Substrate	ChGluc 131A	ChGluc 131B	CgGluc 131A	PsGluc 131A	PsGluc 131B	ZtGluc 131A	PaGluc 131A
β-1,4							
CMC	79	127	167	194	1067	64	126
PASC	46	53	39	4	17	33	28
Cellohexaose	144	95	–	35	404	108	–
Cellotetraose	12	12	–	15	62	10	–
Cellotriose	4	3	–	10	44	3	–
Cellobiose	N.D.	N.D.	–	N.D.	N.D.	N.D.	–
β-1,3/1,4							
Barley β-glucan[a]	8	73	8	26	204	7	21
Lichenan[a]	81	105	69	238	1323	74	45
G4A	3	6	–	1	20	1	–
G4B	N.D.	N.D.	–	N.D.	N.D.	N.D.	–
G4C	N.D.	N.D.	–	N.D.	N.D.	N.D.	–
G3A	2	7	–	2	11	N.D.	–
G3B	N.D.	N.D.	–	N.D.	N.D.	N.D.	–
β-1,3							
Curdlan	6	5	10	16	90	1	271
Laminarihexaose	10	30	12	50	328	42	53
Laminaripentaose	7	25	–	3	18	3	–
Laminaritetraose	3	11	–	1	11	1	–
Laminaritriose	4	15	–	2	21	2	–
Laminaribiose	N.D.	N.D.	–	N.D.	N.D.	N.D.	–
β-1,3/β-1,6							
Laminarin[b]	21	220	28	70	615	19	434
β-1,6							
Pustulan	N.D.	N.D.	N.D.	N.D.	N.D.	N.D.	N.D.

a. The primary detectable soluble product was β-1,4 glycosides, and not β-1,3 glycosides

b. Quantification was done only for the β-1,3 oligosaccharides, as other peaks could not be identified based on known standards.

”–“ not determined

N.D. no activity detected or below the detection limit

CMC: Carboxymethylcellulose; PASC: Phosphoric Acid Swollen Cellulose; G4A: Glucosyl-β(1,3)-Glucosyl-β(1,4)-Glucosyl-β(1,4)-Glucose; G4B: Glucosyl-β(1,4)-Glucosyl-β(1,4)-Glucosyl-β(1,3)-Glucose; G4C: Glucosyl-β(1,4)-Glucosyl-β(1,3)-Glucosyl-β(1,4)-Glucose; G3A: Glucosyl-β(1,4)-Glucosyl-β(1,3)-Glucose; G4A: Glucosyl-β(1,3)-Glucosyl-β(1,4)-Glucose.

758 **Figure legends**

759 Fig. 1. Species tree of microorganisms used in this study. The width of lines indicates the number (from
760 0 to 22) of GH131 genes inferred at each node. The circle area indicates the number of GH131 genes
761 in each extant species (from 0 to 9). The numbers on the internal nodes indicate the average of the
762 number of GH131 genes estimated using Notung 2.9. Three potential horizontal gene transfers detected
763 using Notung 2.9, are indicated with blue lines and arrows. Species marked with an asterisk have been
764 manually added with arbitrary branch lengths. Dashed lines indicate lineages without any GH131-
765 coding genes. Lifestyle is indicated with the background colour of each taxon: Arbuscular mycorrhizal
766 (light blue), Animal associated (orange), Ectomycorrhizal (purple), Endophytes (pink), Ericoid
767 mycorrhizal (dark green), Mycetophagous (red), Orchid mycorrhizal (deep purple), Plant pathogen
768 (light green), Saprotroph (yellow).

769 Fig. 2. Reconstruction of the evolutionary history of the GH131 family with Bayesian inference. Interior
770 nodes and branch width represent posterior probabilities. The tree is rooted between the fungal and
771 oomycetes clades. The groups of microorganisms represented are Oomycetes (purple),
772 Pucciniomycotina (Basidiomycota; red), Agaricomycotina (Basidiomycota; orange), Pezizomycotina
773 (Ascomycota; green). The sequences selected for functional characterisation are highlighted in yellow.
774 The only chytrid GH131 is highlighted in light blue. The leaves of the GH131 sequences that in their
775 native form harbour a CBM1 domain are mentioned in parentheses. Only full-length catalytic domains
776 were used for this tree.

777 Fig. 3. Number of GH131-coding genes in fungal pathogens (FP; n=3), plant pathogens (PP; n=29),
778 saprotrophs (S; n=32), plant symbionts including mycorrhizal fungi and endophytes (SB; n=12), and
779 animal (nematodes, insects, and mammals) associated fungi (AA; n=7), among the selected Dikarya
780 species and excluding Saccharomycetes, Schizosaccharomycetes, and Taphrinomycetes. Box plots
781 indicate the median (line), the 25th and 75th percentiles (box), the maximum and minimum values
782 (whiskers), and the mean (x).

Fig. 4. Chromatographic separation and detection using HPAEC-PAD of the products of the enzymatic reaction of GH131s on substrates with different types of bonds: (A) ChGluc131A on PASC; (B) PaGluc131A on curdlan; (C) CgGluc131A on Lichenan; (D) ChGluc131B on G4A (solid) and G3A (dashed); (E) ChGluc131B (solid line) and ZtGluc131A (dashed line) on Laminarin. Circles indicate glucose units; straight line, β-1,4 bonds; slash line (/), β-1,3 bonds; backslash line (\), β-1,6 bonds.

Fig. 5. Relative amounts of the soluble products generated from birch cellulose fibres upon action of CBHI alone, PsGluc131A and both enzymes (A). The endo-action of PsGluc131A on cellulose chains generates more cleaving sites for CBHI of *T. reesei*, which acts progressively from the non-reducing end (B).

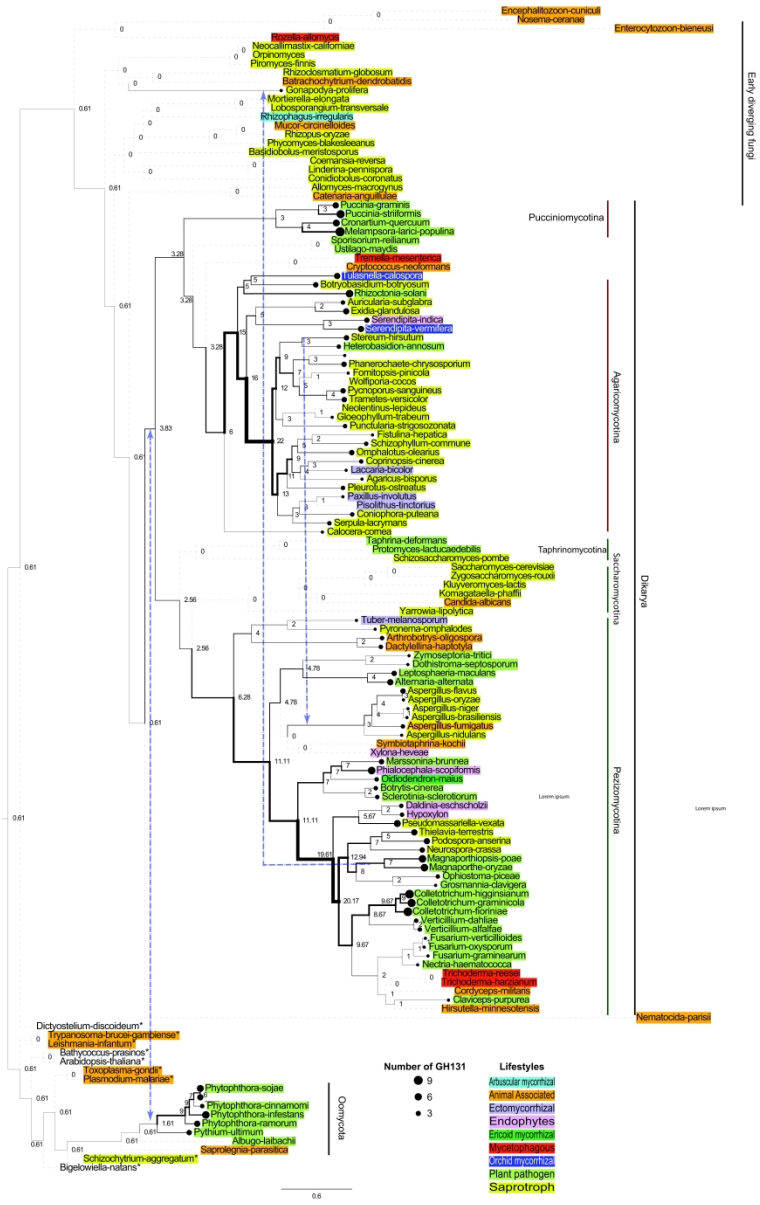

Fig. 1. Species tree of microorganisms used in this study. The width of lines indicates the number (from 0 to 22) of GH131 genes inferred at each node. The circle area indicates the number of GH131 genes in each extant species (from 0 to 9). The numbers on the internal nodes indicate the average of the number of GH131 genes estimated using Notung 2.9. Three potential horizontal gene transfers detected using Notung 2.9, are indicated with blue lines and arrows. Species marked with an asterisk have been manually added with arbitrary branch lengths. Dashed lines indicate lineages without any GH131-coding genes. Lifestyle is indicated with the background colour of each taxon: Arbuscular mycorrhizal (light blue), Animal associated (orange), Ecomycorrhizal (purple), Endophytes (pink), Ericoid mycorrhizal (dark green), Mycetophagous (red), Orchid mycorrhizal (deep purple), Plant pathogen (light green), Saprotroph (yellow).

585x911mm (600 x 600 DPI)

Fig. 2. Reconstruction of the evolutionary history of the GH131 family with Bayesian inference. Interior nodes and branch width represent posterior probabilities. The tree is rooted between the fungal and oomycetes clades. The groups of microorganisms represented are Oomycetes (purple), Pucciniomycotina (Basidiomycota; red), Agaricomycotina (Basidiomycota; orange), Pezizomycotina (Ascomycota; green). The sequences selected for functional characterisation are highlighted in yellow. The only chytrid GH131 is highlighted in light blue. The leaves of the GH131 sequences that in their native form harbour a CBM1 domain are mentioned in parentheses. Only full-length catalytic domains were used for this tree.

585x1124mm (600 x 600 DPI)

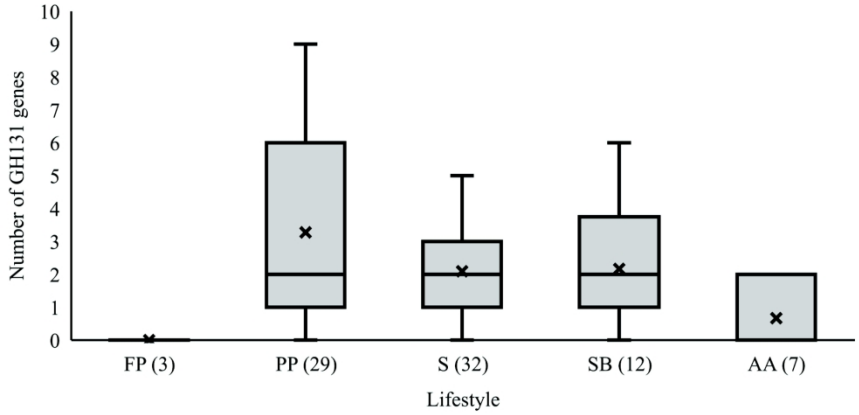

Fig. 3. Number of GH131-coding genes in fungal pathogens (FP; n=3)), plant pathogens (PP; n=29), saprotrophs (S; n=32), plant symbionts including mycorrhizal fungi and endophytes (SB; n=12), and animal (nematodes, insects, and mammals) associated fungi (AA; n=7), among the selected Dikarya species and excluding Saccharomycetes, Schizosaccharomycetes, and Taphrinomycetes. Box plots indicate the median (line), the 25th and 75th percentiles (box), the maximum and minimum values (whiskers), and the mean (x).

279x215mm (300 x 300 DPI)

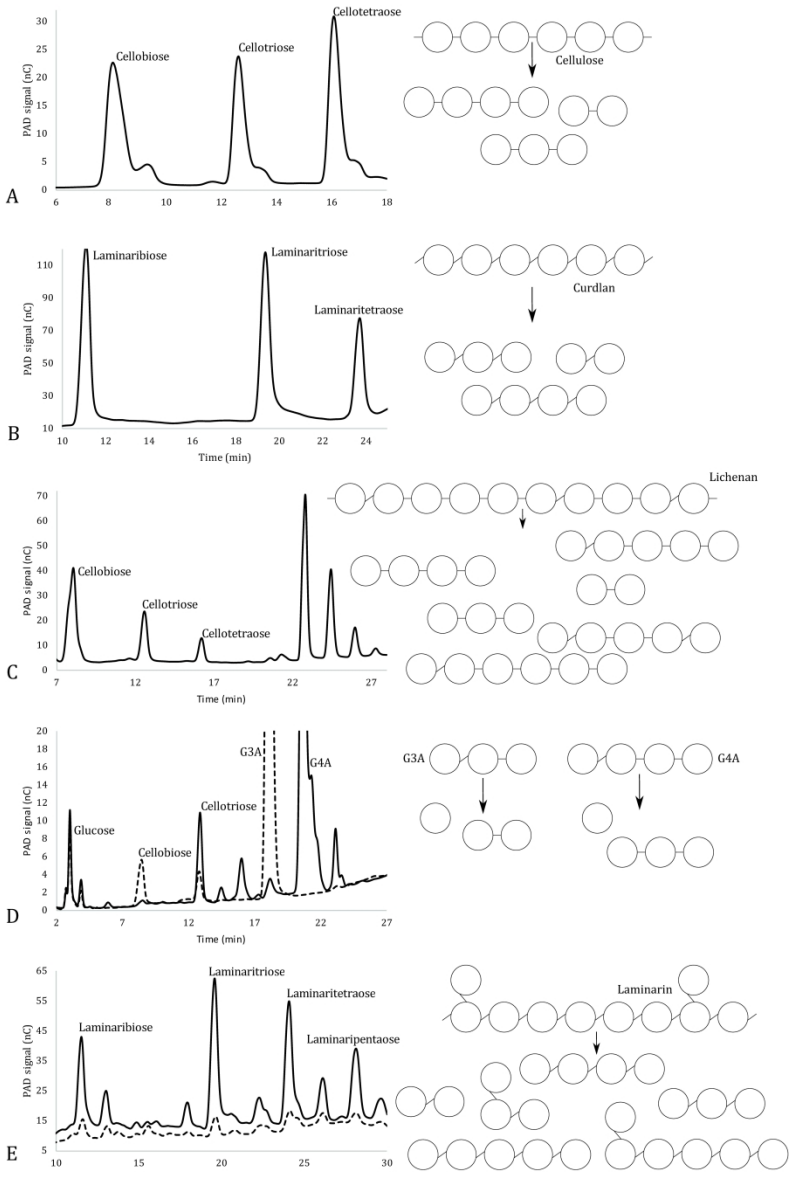

Fig. 4. Chromatographic separation and detection using HPAEC-PAD of the products of the enzymatic reaction of GH131s on substrates with different types of bonds: (A) ChGluc131A on PASC; (B) PaGluc131A on curdlan; (C) CgGluc131A on Lichenan; (D) ChGluc131B on G4A (solid) and G3A (dashed); (E) ChGluc131B (solid line) and ZtGluc131A (dashed line) on Laminarin. Circles indicate glucose units; straight line, β-1,4 bonds; slash line (/), β-1,3 bonds; backslash line (\), β-1,6 bonds.

332x508mm (300 x 300 DPI)

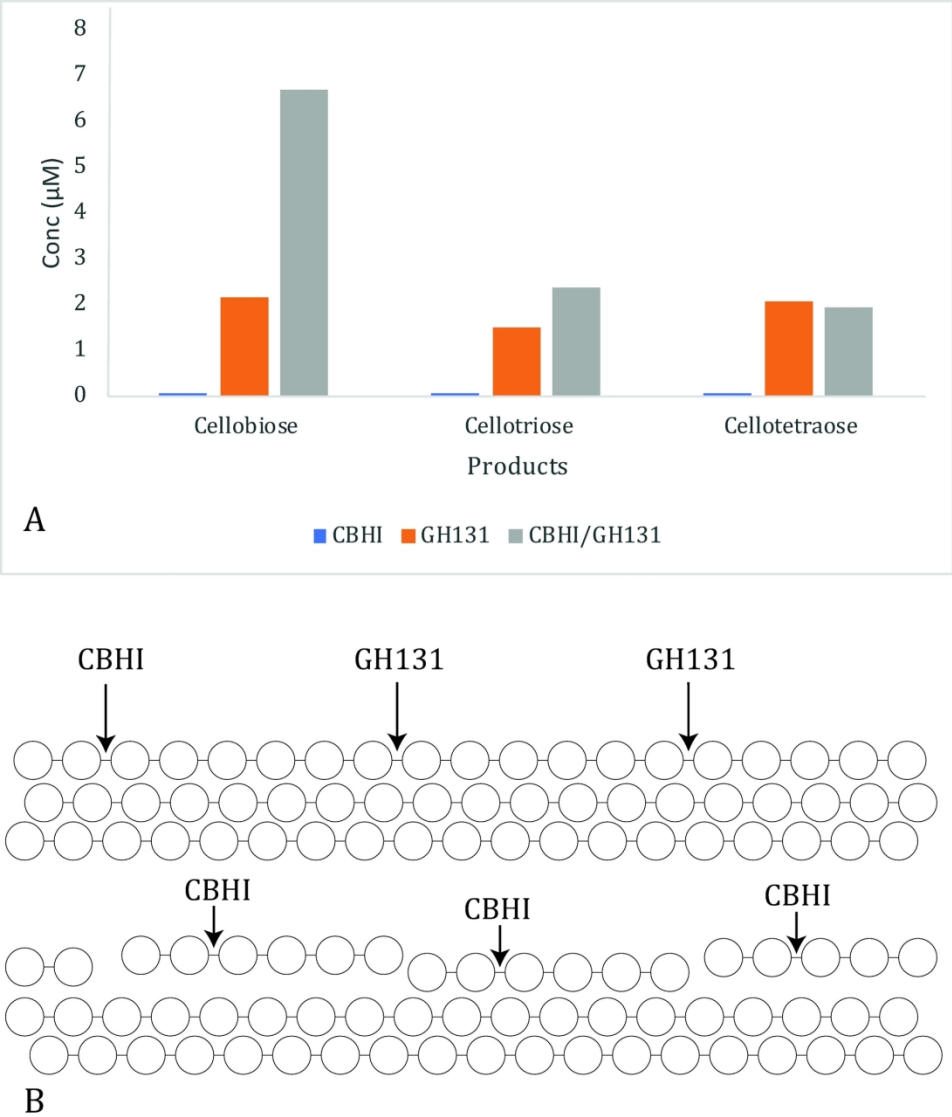

Fig. 5. Relative amounts of the soluble products generated from birch cellulose fibres upon action of CBHI alone, PsGluc131A and both enzymes (A). The endo-action of PsGluc131A on cellulose chains generates more cleaving sites for CBHI of T. reesei, which acts progressively from the non-reducing end (B).

169x212mm (300 x 300 DPI)